Integrating Vegetation Indices and Texture Features from UAV multispectral image for Nondestructive Peanut Aboveground Biomass Estimation

Liya Hu¹, Yueyang Tan¹, Dandan Liu¹, Mingxuan Song¹, Yirou Liu², Juntao Yang^{1*}, Zhenhai Li¹, Bo Bai², Guowei Li²

¹College of Geodesy and Geomatics, Shandong University of Science and Technology, Qingdao 266590, China;

²Institute of Crop Germplasm Resources, Shandong Academy of Agricultural Sciences, Jinan 250100, China;

Keywords: Aboveground biomass, Vegetation Indices, Texture Feature, UAV multispectral images, High-throughput phenotyping monitoring.

Abstract

High-throughput phenotyping monitoring has become increasingly important in modern agriculture, as it can collect plant images to extract and analyse phenotype data related to growth and yield, thereby reducing crop monitoring costs. Aboveground biomass (AGB) is a key indicator for evaluating plant health, growth, and productivity, and reflects the impact of environmental factors (such as water, soil nutrients, and temperature) on plants. However, traditional methods for measuring AGB are often labor-intensive, costly, and limited in spatial coverage. Unmanned aerial vehicles (UAVs)-based remote sensing offer new solutions, enabling large-scale, high-resolution data collection in agricultural fields. Therefore, this study evaluates the use of Vegetation indices (VIs) and Texture features (TFs), as well as their combinations, derived from UAV multispectral imagery to estimate peanut AGB across different growth stages. Specifically, nine VIs and eight TFs with different parameter settings were first derived from RGB and four single-band UAV images. Based on random forest (RF) regression, the study explored the impact of different parameter combinations on the performance of AGB models and analysed the potential of combining VIs and TFs to improve AGB estimation. The results show that TFs effectively complement VIs, significantly enhancing peanut AGB estimation performance. The optimal window size was 7×7, with a direction of 90° and a grey level of 16. The combined VIs and TFs yield a regression with R² and RMSE of 0.929 and 0.032, respectively. These findings suggest that the strategy of extracting image textures and combining features significantly improves the accuracy of AGB estimation, providing a more precise method for monitoring AGB.

1. Introduction

Peanut is a crucial oilseed and economic crop in China, and its high and stable yields is essential for ensuring national oil security and promoting sustainable agricultural development (Bodoira et al., 2022). Aboveground biomass (AGB), a key parameter for assessing growth status of a population, directly reflects plant vigor and nutrient uptake while also indicating overall productivity levels (Morais et al., 2021). Real-time and accurate estimation of peanut AGB is of great significance for guiding precision field management and yield prediction. The traditional AGB estimation methods primarily rely on manual sampling. Although this approach provides accurate AGB, it is destructive, labor-intensive, and time-consuming, making it impractical for large-scale monitoring (Liu et al., 2022). With advancements in sensor technology and intelligent control systems, unmanned aerial vehicle (UAV)-based remote sensing has emerged as a promising tool for large-scale crop phenotyping due to its flexibility, efficiency, and ability to capture high spatiotemporal resolution imagery at a low cost (Bhandari et al., 2020, Wang et al., 2021). Consequently, leveraging UAV-based remote sensing for rapid, non-destructive monitoring of peanut AGB has become a hot topic in recent years.

VIs would primarily reflect the differences in reflectance between vegetation and soil background in the visible and near-infrared spectral bands, which quantitatively assess vegetation growth under certain conditions (Masenyama et al., 2022). In remote sensing applications, VIs have been widely used for estimations for forests and crops AGB(Mutanga et al., 2023). However, the spectral signals of remote sensing images are often saturated in areas with dense vegetation, which might reduce estimation accuracy(Sharma et al., 2022, Zhang et al., 2020). Since the grey level co-occurrence matrix (GLCM) was proposed for texture analysis (Haralick et al., 1973), researchers have increasingly investigated the application of texture features (TFs)

Based on these advantages, this study proposes a non-destructive peanut AGB estimation method that integrates VIs and TFs using UAV multispectral imagery. The experiment involved calculating VIs and TFs from UAV multispectral image, analysing the correlation between VIs and peanut AGB, and investigating the impact of GLCM parameters on AGB estimation. Furthermore, using a random forest (RF) algorithm, different feature sets were compared to evaluate their performance in estimating peanut AGB, ultimately developing an optimal model.

2. Materials and Methods

2.1 Description of Study Site

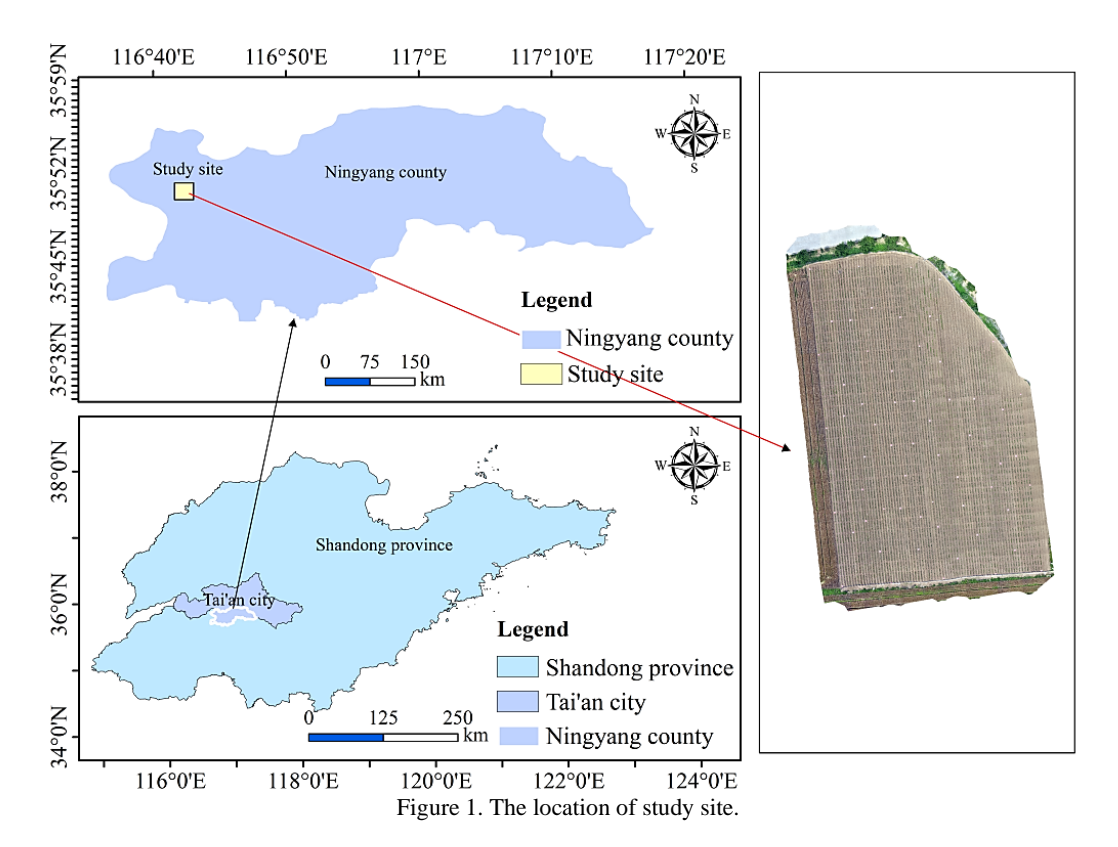
The experimental site is located in Wangbian Community, Ningyang County, Tai'an City, Shandong Province (116°40'48" E, 35°47'47"N), as shown in Fig. 1. Ningyang County falls within a warm temperate humid seasonal climate zone, characterized by distinct four seasons.

2.2 Data Set

2.2.1 Peanut AGB and Remote Sensing Data: The experimental field consisted of 43 independent plots. Sampling and data collection were carried out at four critical growth stages of peanut: seedling, flowering, pod-setting, and maturity.

for AGB estimation (Zhu et al., 2021, Xu et al., 2022). TFs would usually describe the microstructural characteristics of vegetation (Fu et al., 2021). As a complement to VIs in AGB estimation, they effectively mitigate the impact of spectral saturation in later growth stages, thereby improving AGB estimation accuracy(Zheng et al., 2020).

^{*} Correspondence author. E-mail: jtyang@sdust.edu.cn



In each plot, six representative peanut plants were randomly selected. Roots were removed, and the plants were thoroughly washed to eliminate soil and other contaminants, ensuring the accuracy of subsequent measurements. The processed samples were sealed in airtight bags to prevent moisture loss or contamination, then oven-dried at a constant temperature until a stable weight was reached. The dry weight of each sample was measured using a precision electronic balance and carefully recorded. The total dry weight across all plots was obtained by summing the dry weights from each plot. Considering the specific planting density of each plot, the data were further standardized and converted into AGB kg/m².

The UAV (DJI Mavic 3 Enterprise) equipped with a multispectral sensor was used to capture remote sensing images of the field on June 7, June 12, July 5, and July 20, 2023, all under clear and cloud-free conditions between 10:00 and 14:00. The UAV recorded reflectance data in the green, red, red-edge, and near-infrared bands. Additionally, RGB and multispectral images were mosaicked and preprocessed for further analysis.

2.2.2 Vegetation Index Extraction: The VIs are metrics derived from multiple spectral bands to quantify vegetation characteristics. In this experiment, nine VIs were calculated using reflectance values from the UAV green, red, red-edge, and near-infrared bands, along with the blue band from the RGB images. The selected indices (see in Table 1) include Difference Vegetation Indice (DVI), Green Normalized Difference Vegetation Indice (GNDVI), Modified Soil Adjusted Vegetation Indice (MSAVI), Normalized Difference Red-Edge indices (NDRE), Normalized Difference Vegetation Indice (NDVI), Normalized Difference Vegetation Indice (NIRv), Optimized Soil Adjusted Vegetation Indice (OSAVI), Ratio Vegetation Indice (RVI), and Soil-Adjusted Vegetation Indice (SAVI). The VIs for each sampled plot were computed as the average value of all pixels within the plot.

2.2.3 Texture Feature Calculation: Texture is a visual feature that reflects homogeneous patterns in an image, revealing the spatial distribution and structural characteristics of vegetation (Luo et al., 2022). The GLCM is a widely used to extract TFs in image processing, which analyses the spatial relationships between pixels (Niu et al., 2024). In this experiment, the GLCM was applied to extract eight TFs from the UAV green band. The parameters were set as follows: three window sizes (3×3 , 5×5 , and 7×7), four directions (0° , 45° , 90° , and 135°), and three grey levels (16, 32, and 64). The eight TFs (see in Table2) were Contrast, Correlation, Dissimilarity, Entropy, Homogeneity, Mean, Second Moment, and Variance.

VIs	Formula
DVI	$ ho_{NIR}- ho_{Red}$
GNDVI	$rac{(ho_{NIR}- ho_{Green})}{(ho_{NIR}+ ho_{Green})}$
MSAVI	$\frac{2\rho_{NIR} + 1 - \sqrt{(2\rho_{NIR} + 1)^2 - 8(\rho_{NIR} - R)}}{2}$
NDRE	$\frac{\left(\rho_{NIR}-\rho_{Red}-\rho_{RedEdge}\right)}{\left(\rho_{NIR}+\rho_{Red}-\rho_{RedEdge}\right)}$
NDVI	$rac{(ho_{NIR}- ho_{Red})}{(ho_{NIR}+ ho_{Red})}$
NIRv	$NDVI \times \rho_{NIR}$
OSAVI	$\frac{1.16 * (\rho_{NIR} - \rho_{Red})}{(\rho_{NIR} + \rho_{Red} + X)}; X = 0.16$
RVI	$rac{ ho_{NIR}}{ ho_{Red}}$
SAVI	$\frac{\rho_{NIR} - \rho_{Red}}{\rho_{NIR} + \rho_{Red} + L} (1 + L); L = 0.5$

Table 1. Vegetation indices formula

TFs	Formula
Contrast	$\sum_{i,j=0}^{N-1} i P_{i,j} (i-j)^2$
Correlation	$\sum_{i,j=0}^{N-1} P_{i,j} \left[\frac{(i-\mu_x)(i-\mu_y)}{\sigma_x \sigma_y} \right]$
Dissimilarity	$\sum\nolimits_{i,j=0}^{N-1} i P_{i,j} i-j $
Homogeneity	$\sum_{i,j=0}^{N-1} i \frac{P_{i,j}}{1 + (i-j)^2}$
Entropy	$\sum\nolimits_{i,j=0}^{N-1} iP \left(-\ln P_{i,j}\right)$
Mean	$\sum\nolimits_{i,j=0}^{N-1}iP_{i,j}$
Variance	$\sum\nolimits_{i,j=0}^{N-1} i P_{i,j} (i-\mu)^2$
Second Moment	$\sum\nolimits_{i,j=0}^{N-1} P_{i,j}$

Table 2. Texture features formula

2.3 Methods

2.3.1 Feature Selection: Although research on VIs is relatively well-established, the optimal indices for estimating peanut AGB remain unclear. Therefore, this study employs Pearson correlation analysis to identify the most suitable input variables for peanut AGB estimation based on previous research findings and empirical knowledge.

Pearson correlation analysis is a statistical method used to measure the strength of the linear relationship between two variables (Stoica and Babu, 2024) The correlation coefficient (r) ranges from -1 to 1, where the absolute value of r indicates the strength of the linear relationship. When r is close to 1, it indicates a positive correlation between the two variables; conversely, it indicates the existence of a negative correlation; and when the absolute value of r is close to 0, it indicates the existence of a weak correlation between the two variables

Peanut AGB Retrieval Models: Random Forest (RF) is a regression model based on ensemble learning (Breiman, 2001). It effectively captures the complex nonlinear relationships between biomass and crop growth characteristics(Liu et al., 2023). Compared to traditional single decision trees, RF aggregates predictions from multiple trees, reducing the risk of overfitting while enhancing model stability and accuracy, making it well-suited for crop biomass estimation (Mutanga et al., 2012, Jiang et al., 2019). In the RF regression, each decision tree is trained using bootstrap sampling, where samples are randomly drawn with replacement from the original training dataset. At each split node within a tree, a randomly selected subset of features is considered, increasing model diversity and reducing overfitting (Burdett and Wellen, 2022). The final prediction is obtained by averaging the outputs of all decision trees. If the RF model consists of T trees, the predicted value H(x) is computed

$$H(x) = \frac{1}{T} \sum_{t=1}^{T} h_t(x)$$
 (1)

where x denotes the query sample, $h_t(x)$ denotes the prediction of the t-th decision tree, T denoteos the total number of trees in the forest.

2.3.3 Assessment of Model Performance: In our implementation, the Coefficient of Determination (R²) and Root Mean Squared Error (RMSE) were used to evaluate the performance of the Random Forest (RF) model. Specifically, R² is used to assess the degree of model fit. RMSE measures the accuracy of the model's predictions.

$$R^{2} = 1 - \frac{\sum_{i=1}^{m} (f_{i} - f_{y})^{2}}{\sum_{i=1}^{m} (\bar{y} - y_{i})^{2}}$$
(2)

$$RMSE = \sqrt{\frac{1}{m} \sum_{i=1}^{m} (f_{i-y_1})^2}$$
 (3)

where f_i denotes predicted value for the *i*-th observation, y_i denotes the *i*-th field observation, \bar{y} denotes mean of field values, m denotes number of observations.

3. Results and Analysist

3.1 AGB Estimation from Vegetation Indices

The experiment calculated the correlation between nine VIs and AGB. The results are shown in Fig.2. By observing the scatter plot distribution, it is possible to preliminarily determine whether there is a linear relationship between VIs and AGB, as well as the strength of their correlation. For example, the scatter points of DVI and NIRv are roughly arranged along a straight line, indicating that these two features have a linear relationship with AGB. The scatter distribution and the trend of the green line explain the positive or negative correlation between the VIs and AGB. For instance, there is a positive correlation between DVI and AGB. Conversely, if the trend were reversed, it would indicate a negative correlation. Furthermore, the tighter the scatter points are distributed and the closer they are to the trend line, the stronger the correlation between the VIs and AGB; otherwise, the correlation is weaker. Among the 9 VIs, all showed a positive correlation with AGB. Except for NDRE, the absolute values of the correlation coefficients for the remaining VIs were all greater than 0.8, indicating a strong correlation with peanut AGB. DVI is calculated as the simple difference between NIR and Red reflectance, and it maintains a good linear relationship even under high vegetation cover. NIR reflects the actual near-infrared reflectance, which is directly related to chlorophyll content, canopy structure, and other biophysical parameters. Therefore, compared to the traditional NDVI, these two VIs (DVI and NIRv) demonstrate greater advantages under high LAI or high vegetation coverage conditions. NDRE exhibited the lowest correlation, which may be due to its loss of sensitivity at later growth stages with high vegetation coverage, weakening its response to AGB variations. As a result, the experiment excluded NDRE and used the remaining 8 indices for peanut AGB estimation.

As shown in Figure 3, the RF regression model demonstrates a high level of fit for both the training and test datasets, indicating that the selected eight VIs have strong predictive capability for AGB. The RMSE and R^2 for the two sets are similar, suggesting that the model has good generalization ability without significant overfitting issues. According to regression equation, the slope = 0.940 and intercept = 0.010, indicating that the prediction results have a small deviation from the field values when using this

"Mobile Mapping for Autonomous Systems and Spatial Intelligence", 20-22 June 2025, Xiamen, China

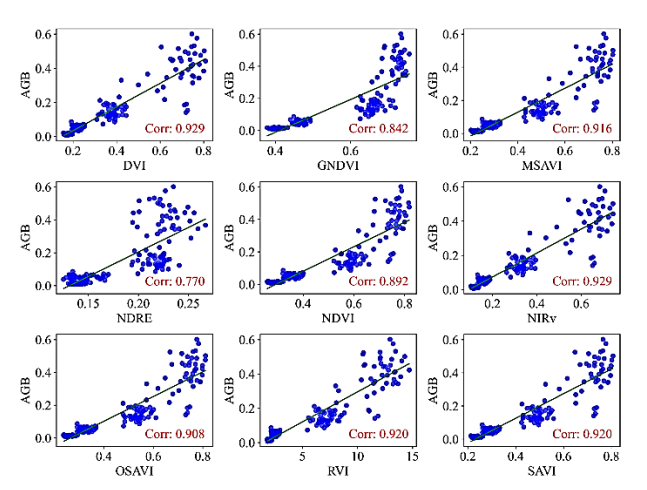


Figure 2. The correlation between VIs and AGB.

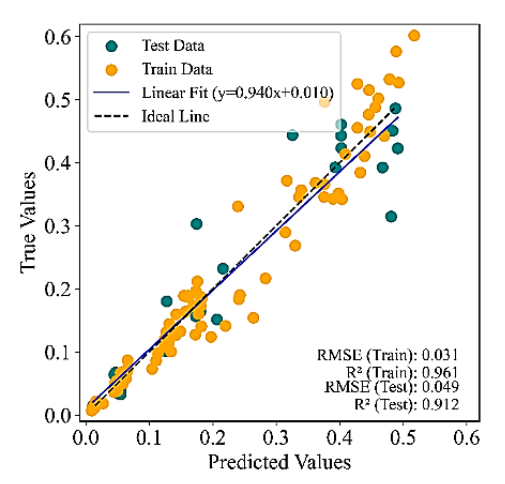


Figure 3. Field versus predicted AGB values based on VIs.

feature set. The black dashed line in the figure represents the ideal line, which almost overlaps with the blue fitted line, and the data points are evenly distributed on both sides of the fitted line. This suggests a strong consistency between the predicted and the field values. The RMSE for the two data sets are 0.031 and 0.049, respectively, indicating that the model's error is low and its predictions are relatively stable. The R² for the training set and test set are 0.961 and 0.912, respectively, demonstrating high accuracy in AGB prediction. Furthermore, the model maintains strong generalization ability, ensuring high stability on the test set. Therefore, VIs provide a reliable indication of AGB, confirming their effectiveness in peanut biomass estimation.

3.2 AGB Estimation from Texture Features

To investigate the impact of GLCM parameters on the enhancement of the RF model and identify the optimal parameter combination, the experiment evaluated 36 different combinations of TF parameters, including window size (3 levels), direction (4 levels), and grey levels (3 levels), for peanut AGB estimation. R^2 and RMSE were used as selection criteria. As illustrated in Fig. 4, the estimation performance of TFs in the training set exhibited no significant variation across different parameters. The overall R^2 exceeded 0.9, and RMSE remained below 0.050, demonstrating that the model performed well on the training set. However, the test set results showed noticeable variations. The combination of a 7×7 window, 90° direction, and 16 grey levels

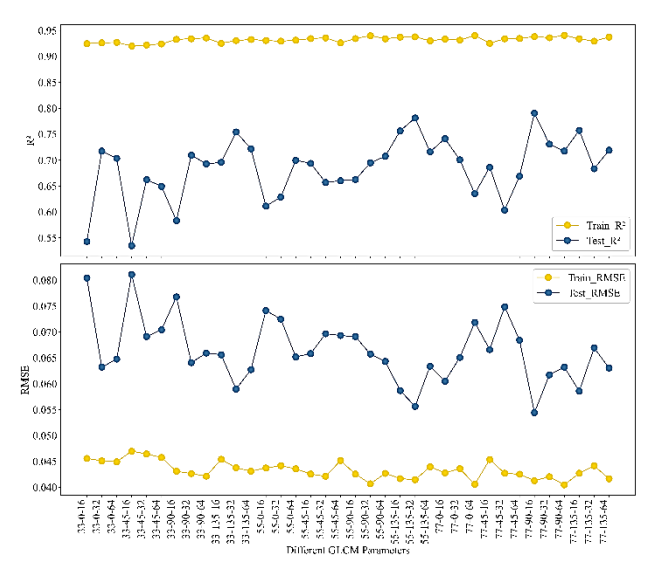


Figure 4. Field versus predicted AGB values based on GLCM TFs.

achieved the best performance, with the highest $\ensuremath{R^2}$ and the lowest RMSE.

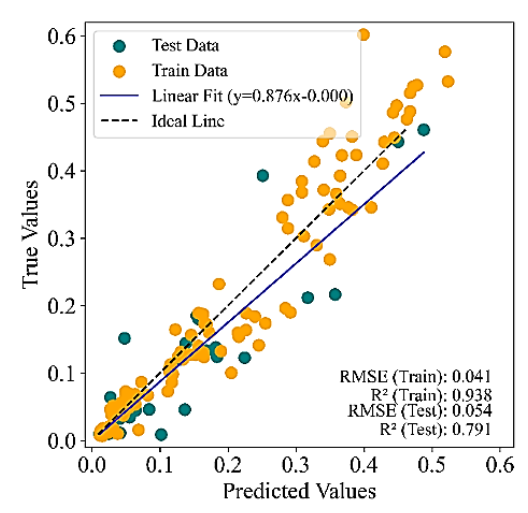


Figure 5. Field versus predicted AGB values based on the optimal TFs.

Fig.5 presents the AGB estimation by using optimal TF combination. The high R^2 for both two data sets indicate that the model effectively predicts peanut AGB. However, the fitting accuracy and performance on the test set are noticeably lower than those on the training set, with $R^2 = 0.79$ and RMSE = 0.054. While these results are within an acceptable range, they suggest that the RF model exhibits a weaker generalization ability on the test set.

Overall, while TFs computed with different parameters can be used for AGB estimation, the experimental results did not reach the same level of accuracy as VIs and fell short of the desired estimation goal.

3.3 AGB Estimation based on Vegetation and Texture Features

To assess whether combining VIs and TFs can enhance the accuracy of peanut AGB estimation, this study incorporated a

total of 16 features, comprising both VIs and TFs, as input variables for regression. As shown in Fig.6, compared to models using only a single type of feature, the current model exhibits a significant improvement in both R² and RMSE metrics. Most data points align closely with the black ideal line, indicating a high level of consistency between the predicted and actual values. Both the training and test datasets exhibit a strong linear trend, demonstrating the model's excellent fit. The intercept is 0.004, which is close to zero, indicating minimal systematic bias. The R² values for the training and test sets are 0.969 and 0.929, respectively, demonstrating the model's ability to effectively explain AGB variability while maintaining strong generalization capability.

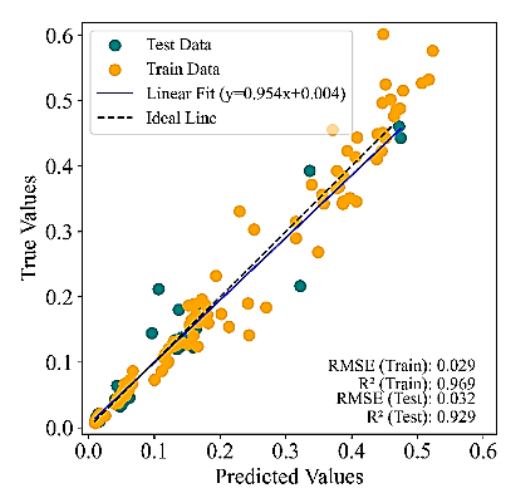


Figure 6. Field versus predicted biomass values based on VIs+TFs.

Input	Test	Test
VIs	0.912	0.049
TFs	0.791	0.054
VIs+TFs	0.929	0.032

Table 3. Results of different feature sets

Table 3 summarizes the performance of three different input feature sets in predicting peanut AGB. The combination of VIs and TFs achieved the highest test set R² of 0.929, making an improvement of 1.86% and 17.59% compared to using only VIs or TFs, respectively. Moreover, this combination resulted in the lowest test set RMSE of 0.032, reducing errors by 34.69% and 40.74% compared to VIs or TFs alone. These findings highlight that integrating VIs and TFs forms the optimal feature set, delivering more accurate and stable predictions than relying on a single feature type. The inclusion of TFs as a complementary variable to VIs significantly improves the accuracy of AGB prediction.

4. Discussion

In precision agriculture and ecological monitoring, remote sensing has become a crucial method for estimating crop AGB. Due to its computational efficiency and sensitivity to crop growth status, remote sensing techniques have been widely applied in AGB estimation. In this study, Pearson correlation analysis revealed a strong correlation between VIs and peanut AGB. A peanut AGB estimation model was constructed by using 8 VIs, achieving R² and RMSE of 0.912 and 0.049, respectively. These

results confirm that VIs play a crucial role in peanut AGB estimation.

The predictive accuracy of the RF model is optimized when the window size, orientation, and grey levels of the GLCM align well with the spatial structure and spectral characteristics of the crop targets. A window size that is too small may fail to capture local details, resulting in insufficient differentiation of texture features within the peanut canopy structure. Conversely, an excessively large window may obscure critical details such as leaf distribution and inter-row plant variations. The smallest window size (3×3) did not yield the best peanut AGB estimation performance (Fig.4), a result consistent with findings from previous studies (Liu et al., 2023), who reported that window (7×7) provided the optimal estimation performance for rice AGB throughout the growing season. Peanut plants exhibit lowgrowing, prostrate growth characteristics, forming a dense vegetation layer that extensively covers the ground surface. When the window size is too small, the extracted TFs fail to capture the macro-structural characteristics of peanut plants effectively. A 7×7 window size enables the capture of global information while minimizing background soil interference, allowing for a more comprehensive structural description. Peanuts are typically grown in row-based planting patterns, where TFs aligned with row directions (0° or 90°) provide more effective information capture. In this study, under the 7×7 window configuration, TFs extracted at 90°, which closely aligns with the planting row direction—yielded the best performance, whereas 45° resulted in the poorest outcomes. This discrepancy may be attributed to the decreasing inter-row gaps as peanut AGB increases, where TFs parallel to planting rows more effectively capture these structural changes, thereby enhancing the accuracy of peanut AGB estimation. Grey levels influence the granularity of GLCM calculations. Previous studies on grey-level selection have been limited. In peanut canopy texture analysis, 16 grey levels effectively retain texture contrast and capture pixel variations without excessively segmenting grey values, which could otherwise disperse the extracted features. These findings underscore the significant impact of GLCM parameter selection on the predictive performance of the RF model.

As shown in Table 3, the estimation accuracy of peanut AGB significantly improves when VIs and TFs are combined compared to using a single feature type. In remote sensing-based crop AGB estimation, VIs and TFs serve as two complementary sources of information. VIs would primarily capture spectral characteristics. For example, NDWI reflects plant water status, which indirectly influences peanut growth and final biomass. However, at high biomass levels, the estimation accuracy of VIs may be affected by saturation effects. In contrast, TFs provide insights into crop canopy structure, uniformity, and growth variability. For instance, which quantifies the dispersion of pixel values, effectively differentiates between high- and low-biomass regions. However, since TFs are derived from image greyscale distributions, they do not directly reflect the physiological and biochemical properties of vegetation. By integrating VIs and TFs, the peanut AGB estimation model achieves the best fitting performance and estimation accuracy, with R2 =0.929 and RMSE = 0.032. These results confirm that combining VIs and TFs is the optimal approach for accurately retrieving peanut AGB.

5. Summary and Outlook

Accurately assessing peanut above-ground biomass (AGB) provides valuable insights for estimating and managing crop health and productivity. This study, focusing on field-grown peanuts, developed models based on three different feature sets

(VIs, TFs, and VIs + TFs) demonstrating the strong potential of VIs for AGB estimation.

Importantly, the three core parameters of the GLCM are interrelated rather than independent. A comprehensive evaluation of various TFs was conducted to identify optimal GLCM configurations for AGB estimation, with results indicating that a 7×7 window, 90° orientation, and 16 grey levels yielded the best performance. By incorporating TFs, the study effectively mitigated the spectral saturation problem commonly associated with VIs. The integration of VIs and TFs not only demonstrated the feasibility of using combined features for AGB estimation but also significantly improved prediction accuracy. This integrated approach provides a promising pathway for crop monitoring in precision agriculture.

However, several challenges remain. The reliance on UAV-derived data introduces sensitivity to weather conditions, such as cloud cover and wind, which can impact data acquisition quality and consistency. Additionally, the manual delineation of sample plots, while ensuring accuracy, is labor-intensive and may limit scalability in large-scale agricultural applications.

In future work, we aim to address these limitations by automating sampling processes and exploring the use of additional spectral inputs beyond the green band, such as red-edge or near-infrared wavelengths, which have the potential to further enhance model robustness and accuracy under diverse field conditions.

Acknowledgements

This work was jointly funded by the Shandong Provincial Key Research and Development Program (grant numbers 2022LZGC021 and 2021LZGC026), the Higher Education Institutions Youth Innovation and Science & Technology Support Program of Shandong Province under Grant 2024KJH062.

References

Bhandari, M., Ibrahim, A. M., Xue, Q., Jung, J., Chang, A., Rudd, J. C., Maeda, M., Rajan, N., Neely, H. & Landivar, J. 2020. Assessing winter wheat foliage disease severity using aerial imagery acquired from small Unmanned Aerial Vehicle (UAV). *Computers and Electronics in Agriculture*, 176, 105665

Bodoira, R., Cittadini, M. C., Velez, A., Rossi, Y., Montenegro, M., Martínez, M. & Maestri, D. 2022. An overview on extraction, composition, bioactivity and food applications of peanut phenolics. *Food chemistry*, 381, 132250

Breiman, L. 2001. Random forests. *Machine learning*, 45, 5-32 Burdett, H. & Wellen, C. 2022. Statistical and machine learning methods for crop yield prediction in the context of precision agriculture. *Precision agriculture*, 23, 1553-1574

Fu, Y., Yang, G., Song, X., Li, Z., Xu, X., Feng, H. & Zhao, C. 2021. Improved estimation of winter wheat aboveground biomass using multiscale textures extracted from UAV-based digital images and hyperspectral feature analysis. *Remote Sensing*, 13, 581

Haralick, R. M., Shanmugam, K. & Dinstein, I. H. 1973. Textural features for image classification. *IEEE Transactions on systems, man, and cybernetics*, 610-621

Jiang, Q., Fang, S., Peng, Y., Gong, Y., Zhu, R., Wu, X., Ma, Y., Duan, B. & Liu, J. 2019. UAV-based biomass estimation for rice-combining spectral, TIN-based structural and meteorological features. *Remote Sensing*, 11, 890

Liu, J., Zhu, Y., Song, L., Su, X., Li, J., Zheng, J., Zhu, X., Ren, L., Wang, W. & Li, X. 2023. Optimizing window size and directional parameters of GLCM texture features for estimating rice AGB based on UAVs multispectral imagery. *Frontiers in Plant Science*, 14, 1284235

Liu, Y., Feng, H., Yue, J., Li, Z., Yang, G., Song, X., Yang, X. & Zhao, Y. 2022. Remote-sensing estimation of potato above-ground biomass based on spectral and spatial features extracted from high-definition digital camera images. *Computers and Electronics in Agriculture*, 198, 107089

Luo, S., Jiang, X., He, Y., Li, J., Jiao, W., Zhang, S., Xu, F., Han, Z., Sun, J. & Yang, J. 2022. Multi-dimensional variables and feature parameter selection for aboveground biomass estimation of potato based on UAV multispectral imagery. *Frontiers in Plant Science*, 13, 948249

Masenyama, A., Mutanga, O., Dube, T., Bangira, T., Sibanda, M. & Mabhaudhi, T. 2022. A systematic review on the use of remote sensing technologies in quantifying grasslands ecosystem services. *GIScience & Remote Sensing*, 59, 1000-1025

Morais, T. G., Teixeira, R. F., Figueiredo, M. & Domingos, T. 2021. The use of machine learning methods to estimate aboveground biomass of grasslands: A review. *Ecological indicators*, 130, 108081

Mutanga, O., Adam, E. & Cho, M. A. 2012. High density biomass estimation for wetland vegetation using WorldView-2 imagery and random forest regression algorithm. *International Journal of Applied Earth Observation and Geoinformation*, 18, 200, 406

Mutanga, O., Masenyama, A. & Sibanda, M. 2023. Spectral saturation in the remote sensing of high-density vegetation traits: A systematic review of progress, challenges, and prospects. *ISPRS Journal of Photogrammetry and Remote Sensing*, 198, 297-309

Niu, Y., Song, X., Zhang, L., Xu, L., Wang, A. & Zhu, Q. 2024. Enhancing Model Accuracy of UAV-Based Biomass Estimation by Evaluating Effects of Image Resolution and Texture Feature Extraction Strategy. *IEEE Journal of Selected Topics in Applied Earth Observations and Remote Sensing*,

Sharma, P., Leigh, L., Chang, J., Maimaitijiang, M. & Caffé, M. 2022. Above-ground biomass estimation in oats using UAV remote sensing and machine learning. *Sensors*, 22, 601

Stoica, P. & Babu, P. 2024. Pearson–Matthews correlation coefficients for binary and multinary classification. *Signal Processing*, 222, 109511

Wang, T., Liu, Y., Wang, M., Fan, Q., Tian, H., Qiao, X. & Li, Y. 2021. Applications of UAS in crop biomass monitoring: A review. *Frontiers in Plant Science*, 12, 616689

Xu, L., Zhou, L., Meng, R., Zhao, F., Lv, Z., Xu, B., Zeng, L., Yu, X. & Peng, S. 2022. An improved approach to estimate ration rice aboveground biomass by integrating UAV-based

ISPRS Annals of the Photogrammetry, Remote Sensing and Spatial Information Sciences, Volume X-1/W2-2025
13th International Conference on Mobile Mapping Technology (MMT 2025)
"Mobile Mapping for Autonomous Systems and Spatial Intelligence", 20–22 June 2025, Xiamen, China

spectral, textural and structural features. $Precision\ Agriculture$, 23, 1276-1301

Zhang, M., Zhou, J., Sudduth, K. A. & Kitchen, N. R. 2020. Estimation of maize yield and effects of variable-rate nitrogen application using UAV-based RGB imagery. *biosystems engineering*, 189, 24-35

Zheng, H., Ma, J., Zhou, M., Li, D., Yao, X., Cao, W., Zhu, Y. & Cheng, T. 2020. Enhancing the nitrogen signals of rice canopies

across critical growth stages through the integration of textural and spectral information from unmanned aerial vehicle (UAV) multispectral imagery. *Remote Sensing*, 12, 957

Zhu, W., Sun, Z., Huang, Y., Yang, T., Li, J., Zhu, K., Zhang, J., Yang, B., Shao, C. & Peng, J. 2021. Optimization of multi-source UAV RS agro-monitoring schemes designed for field-scale crop phenotyping. *Precision Agriculture*, 22, 1768-1802